AJChE 2017, Vol. 17, No. 1, 73 – 81

Numerical Study of Fluid Dynamics in Suspension Culture of iPS Cells

Masaki Yano [1]
Takuya Yamamoto [1]
Yasunori Okano [1]
Toshiyuki Kanamori [2]
Mashiro Kino – oka [3]

[1] *Gradient School of Engineering Science, Osaka University, Machikaneyama 1-3, Toyonaka, Osaka 560-8531, Japan*

[2] *Biotechnology Research Institute for Drug Discovery, National Institute of Advanced Industrial Science and Technology (AIST) Tsukuba Center 5th, 1-1-1 Higashi, Tsukuba, Ibaraki 305-8565, Japan*

[3] *Gradient School of Engineering, Osaka University, Yamadaoka 2-1, Suita, Osaka 565-0871, Japan*

[*] *e-mail:* y.masaki@cheng.es.osaka-u.ac.jp

In a suspension culture of iPS cells, the shear stress generated during mixing is expected to promote differentiation of induced pluripotent stem (iPS) cells. The stress on the cells can be controlled by rotational rate and shape of impeller. However, it is difficult to optimize these operative parameters by experiments. Therefore, we have developed a numerical model to obtain the average and the maximum shear stress in two kinds of stirred tanks and an orbital shaking cylindrical container. The present results showed that the shear stress strongly depended on the type of mixing and lesser extent on the shape of the impeller. The average shear stress is larger in the shaking mode than that in the stirring mode. In contrast, the maximum shear stress is much smaller in the shaking than the stirring. These results suggest that stirring and shaking should be selectively used depending on the application.

Keywords: iPS cell, suspension culture, shear stress, numerical simulation, stirred tank, orbital shaking cylindrical container

INTRODUCTION

Induced pluripotent stem (iPS) cells have the ability to become various kinds of cells and proliferate almost infinitely (Takahashi *et al.* 2007). Therefore, they are expected to play an important role in the field of regenerative medicine. However, producing a large organ needs 10^8-10^9 iPS cells (Olmer *et al.* 2012) and the current method of cultivation by manual operation in a static culture cannot meet this demand. Hence, it is essential to develop a new culture method that can produce inexpensively a large number of iPS cells while maintaining the undifferentiated state. One way to achieve this is by substitution of static culture with

suspension culture.

In the cell suspension culture, it is important to know the suitability and impact of mixing on the cell culture. Particularly, it is important to maintain the undifferentiated state of the iPS cells since the deviation from the undifferentiated state leads to loss of the self-renewal ability and pluripotency of the iPS cells. In the case of mouse embryonic stem cells, the number of differentiated cells has been found to increase when the shear stress on the cells (Adamo *et al.* 2009) and the number of blade rotations during stirring were increased (Sargent *et al.* 2012). iPS cells are also expected to behave in a similar way.

There are many parameters in the suspension culture, such as mode of mixing (stirring and shaking), mixing speed, tank scale, physical properties of medium, etc., which also affect the cell culture and shear stress. Experimental studies on the effect of single parameter have been performed. Olmer *et al.* (2010) have investigated the effect of the impeller design, and the influence of the properties of the culture fluid has been studied by Otsuji *et al.* (2014). Practical application of the suspension culture of iPS cells, however, requires optimization of the full set of parameters, which is difficult to achieve by experiments alone. Therefore, numerical simulation must be a powerful tool for understanding the main factors for the suspension culture. On the other hand, to the best of the authors' knowledge, there is no literature on the numerical simulation of suspension culture of iPS cells.

A numerical model has been developed to obtain the shear stress acting on the particles in a stirred tank coupling computational fluid dynamics (CFD) and discrete element method (DEM) in the field of crystal growth (Ali *et al.* 2015). Investigations performed in a shaken cylindrical container coupling CFD-DEM and volume of fluid (VOF) method (Jing *et al.* 2016, Salek *et al.* 2012) have also been reported.

In this study, we have developed the numerical model to obtain the average and the maximum shear stress acting on the cells in a stirred tank and an orbital shaken cylindrical container for suspension culture of iPS cell. In the present simulations, we calculated the behavior of cell culture including the movement of iPS cells that are affected by drag force, collision with wall and gravitation. Since iPS cells form a spherical colony, we assumed the colony of iPS cells to be a sphere. Therefore, CFD and DEM are coupled to simulate stirring; CFD, DEM and VOF are coupled to simulate shaking in OpenFOAM, which is an open source CFD package.

NUMERICAL ANALYSIS

Computational Condition

The following assumptions were made in the present model to represent the iPS cells: (1) A colony of iPS cells is a solid spherical particle and does not change in size with time. (2) The collisions between particles are neglected since the particle concentration is very low. (3) The collision of a particle with the impeller, the side wall and the bottom wall is perfectly elastic. The kinematic viscosity of culture is 1.1×10^{-6} m^2/s, the specific gravity of particles used is 1.005, the particle

diameter is 1mm and the total number of particles is 208 in stirring and 196 in shaking. On the wall, no-slip condition is imposed on the flow velocity.

Stirring

We coupled CFD with DEM. A one-way coupling approach was used, that is, the movement of particles is affected by the fluid flow but the fluid flow is not affected by particles' motion. The particle-particle interaction is neglected.

DEM Equations

DEM is utilized to calculate the movement of particles. In this approach, the motion of each particle is governed by the Newton's second law of motion:

$$m_{\mathrm{s}} \frac{\partial \boldsymbol{v}_{\mathrm{s}}}{\partial t} = \boldsymbol{F}_{\mathrm{D}} + \boldsymbol{F}_{\mathrm{g}} \tag{1}$$

where m is mass, $\boldsymbol{v}$ is velocity, t is time. $\boldsymbol{F}_{\mathrm{D}}$ is drag force and $\boldsymbol{F}_{\mathrm{g}}$ is gravitational force expressed as

$$\boldsymbol{F}_{\mathrm{g}} = m_{\mathrm{s}} \boldsymbol{g} (1 - \frac{\rho_{\mathrm{f}}}{\rho_{\mathrm{s}}}) \tag{2}$$

$$\boldsymbol{F}_{\mathrm{D}} = C_{\mathrm{D}} A_{\mathrm{p}} \frac{\rho_{\mathrm{f}} \, | \boldsymbol{v}_{\mathrm{f}} - \boldsymbol{v}_{\mathrm{s}} |^2}{2} \frac{\boldsymbol{v}_{\mathrm{f}} - \boldsymbol{v}_{\mathrm{s}}}{| \boldsymbol{v}_{\mathrm{f}} - \boldsymbol{v}_{\mathrm{s}} |} \tag{3}$$

where ρ is density, A_{p} is projected area, C_{D} is drag coefficient.

$$C_{\mathrm{D}} = \begin{cases} \dfrac{24}{Re_{\mathrm{par}}} (1 + \dfrac{1}{6} Re_{\mathrm{par}}{}^{\frac{2}{3}}) & Re_{\mathrm{par}} < 1000 \\ 0.424 & Re_{\mathrm{par}} \geq 1000 \end{cases} \tag{4}$$

$$Re_{\mathrm{par}} = \frac{\rho_{\mathrm{f}} \, | \boldsymbol{v}_{\mathrm{f}} - \boldsymbol{v}_{\mathrm{s}} | \, d_{\mathrm{s}}}{\mu_{\mathrm{f}}} \tag{5}$$

Re_{par} is Reynords number of particle, d is diameter, μ is viscosity. The suffixes s and f stand for solid and fluid, respectively.

CFD Equations

CFD is adopted to calculate the fluid flow. A sliding mesh technique is employed to simulate the rotating impeller. The motion of fluid is governed by the equations of continuity and Navier-stokes:

$$\frac{\partial \rho_{\mathrm{f}}}{\partial t} + \nabla \cdot (\rho_{\mathrm{f}} \boldsymbol{v}_{\mathrm{f}}) = 0 \tag{6}$$

$$\frac{\partial}{\partial t} (\rho_{\mathrm{f}} \boldsymbol{v}_{\mathrm{f}}) + \nabla \cdot (\rho_{\mathrm{f}} \boldsymbol{v}_{\mathrm{f}} \boldsymbol{v}_{\mathrm{f}}) = -\nabla p + \nabla \cdot (\mu_{\mathrm{f}} \nabla \boldsymbol{v}_{\mathrm{f}}) + \rho_{\mathrm{f}} \boldsymbol{g} \tag{7}$$

Shaking

We coupled CFD-DEM with VOF to model free surface. Governing equations of DEM and CFD are similar to the case of stirring.

DEM Equations

$$m_{\mathrm{s}} \frac{\partial \boldsymbol{v}_{\mathrm{s}}}{\partial t} = \boldsymbol{F}_{\mathrm{D}} + \boldsymbol{F}_{\mathrm{g}} - m_{\mathrm{s}} \frac{d\boldsymbol{U}}{dt} \tag{8}$$

$$\boldsymbol{U} = \begin{bmatrix} -R_{\mathrm{s}} \omega \sin \omega t \\ -R_{\mathrm{s}} \omega \cos \omega t \\ 0 \end{bmatrix} \tag{9}$$

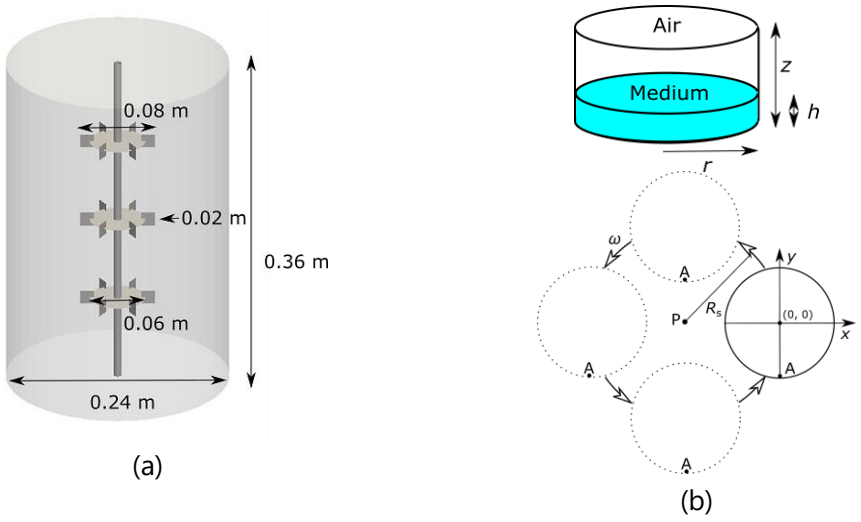

Fig. 1: Figure 1 (a)Numerical configuration of stirring model used for validation. (b) Numerical schematic of shaking model.

CFD Equations

$$\frac{\partial \rho_f}{\partial t} + \nabla \cdot (\rho_f \boldsymbol{v}_f) = 0 \tag{10}$$

$$\frac{\partial}{\partial t}(\rho_f \boldsymbol{v}_f) + \nabla \cdot (\rho_f \boldsymbol{v}_f \boldsymbol{v}_f) = -\nabla p + \nabla \cdot (\mu_f \nabla \boldsymbol{v}_f) + \rho_f \boldsymbol{g} - m_s \frac{d\boldsymbol{U}}{dt} \tag{11}$$

VOF Equation

In the VOF method, fraction function · is defined as α = 1 for fluid, α = 0 for air and 0 < α < 1 for the interface. Algebraic VOF is governed by the following transport equation with the fraction function (Rusche 2002).

$$\frac{\partial \alpha}{\partial t} + \nabla \cdot (\alpha \boldsymbol{v}_f) + \nabla \cdot ((1-\alpha)\alpha \boldsymbol{v}_f) = 0 \tag{12}$$

Discretization and Coupling Units

When we conduct CFD including VOF, the governing equations were discretized by the finite volume method and the velocity and pressure fields were coupled by the PISO algorithm (Issa 1986). The values on cell interfaces were calculated by a second-order linear interpolation scheme. For the discretization of time derivative, the first-order implicit Euler method was applied. In this study, we focused on the effect of shear stress. Therefore, fewer colonies compared to that of the actual experiments in the stirred tank were used, and one-way coupling approach must be reasonable.

RESULTS AND DISCUSSION

Code Validation of Stirring and Shaking

In this study, we compared our numerical results of stirring with those given in Zalc *et al.* in order to validate the numerical code. The numerical domain of the stirring model used for validation is shown in **Figure 1 (a)**. Zalc *et al.* measured vertical and radial velocity components in the vessel for a vertical line halfway to the

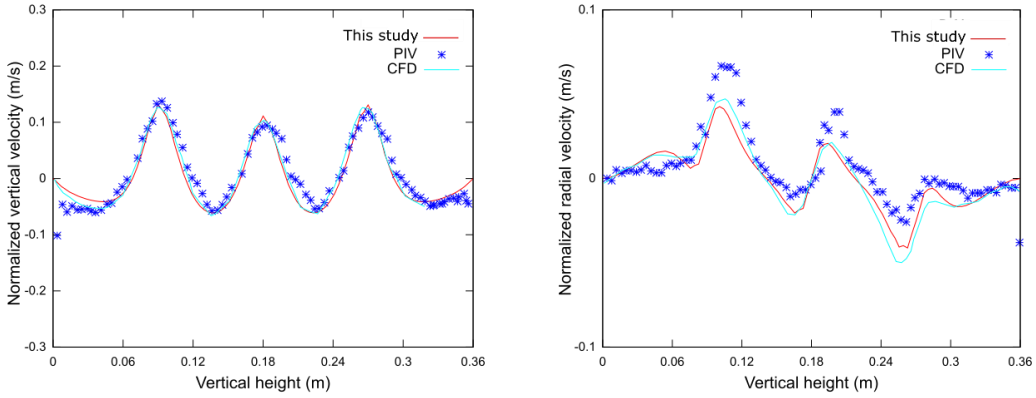

(a) (b)

Fig. 2: Figure 2 Comparison of the present numerical results with PIV and CFD results of Zalc et al. for (a) normalized vertical and (b) radial velocity components vs. vertical height in the vessel for a vertical line halfway to the tank wall, aligned with an impeller blade, and spanning the vessel height.

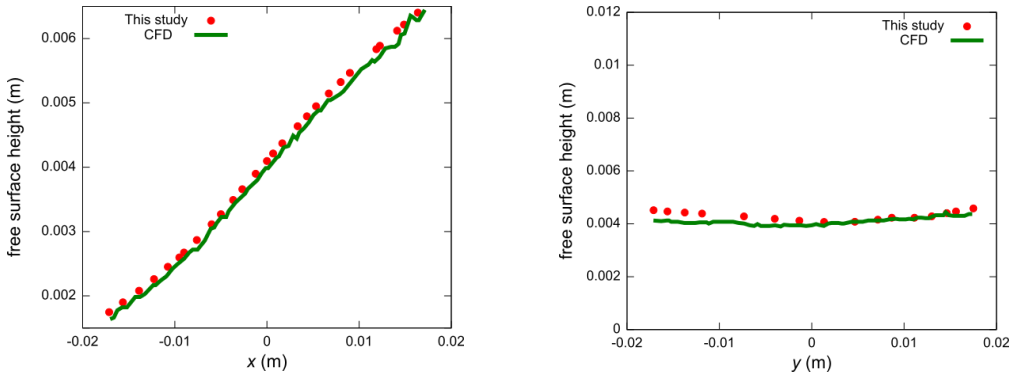

(a) (b)

Fig. 3: Figure 3 Comparison of free surface height of the liquid of the present numerical results with CFD results of Salek et al. along (a) the x-direction and (b) the y-direction

Table 1. Parameters of Numerical Configuration of Shaking Model

	h **(mm)**	***z*** **(mm)**	***r*** **(mm)**	R_s **(mm)**	ω **(rad/s)**
Validation model	4	18	17.5	9.5	10.47

tank wall, aligned with an impeller blade, and spanning the vessel height. These results were compared with the present results as shown in **Figure 2**. In order to validate the simulation code for shaking, numerical simulations by Salek *et al.* were also reproduced. The numerical domain of the shaking model for validation is shown in **Table 1** and **Figure 1 (b)**. The cylinder with radius r is shaken at an angular velocity of ω with P as the center and radius of rotation R_s. The present study focused on the fluid behavior in the orbital shaken bioreactor at 60 rpm and with the initial free surface height with a liquid volume of 4 ml. In the case of shaken reactor, free surface height of the liquid in the cylinder changes. The free surface height of obtained in the present study and by Salek *et al.* are compared in **Figure 3** and y-component of velocity at z = 2 mm are shown in **Figure 4**, and it is found

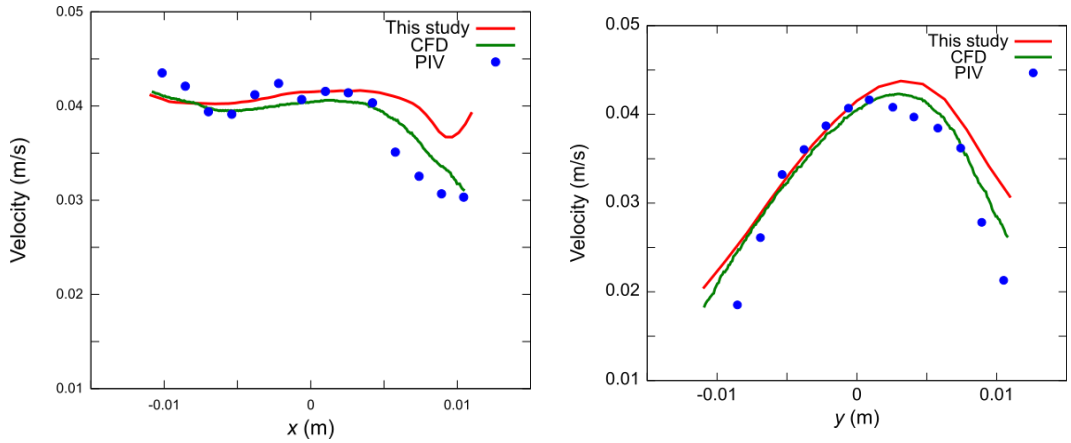

(a) (b)

Fig. 4: Figure 4 Comparison of y-component of velocity of the present numerical results with PIV and CFD results of Salek et al. at z = 2 mm along (a) the x-direction and (b) the y-direction.

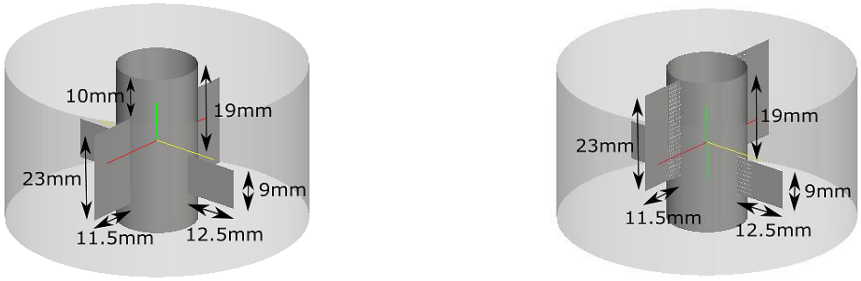

(a) (b)

Fig. 5: Figure 5 Numerical configurations of stirring model: (a) one level (b) two level.

Table 2. Parameters of Numerical Configuration of Shaking 100 mm Dish

	h **(mm)**	***z*** **(mm)**	***r*** **(mm)**	R_s **(mm)**	ω **(rad/s)**
100 mm dish	10	43.2	42	12.5	4.17

that they are good agreement each other.

In this section, we discussed the reliability of the present numerical code in calculating the fluid flow in stirring and shaking. Results showed that the numerical models were developed correctly. Therefore, in the next section, particles are inserted in a stirred tank and an orbital shaken cylindrical container to model actual suspension culture for iPS cells.

One – Level and Two – Level Impeller of Stirring vs Shaking

Numerical configurations of stirring model with two setups of the impellers are shown in **Figure 5**. Numerical configuration of the shaking model was a 100 mm dish with the cylindrical shape similar to that in **Figure 1 (b)**. The geometrical and operative parameters are shown in **Table 2**. For stirring and shaking,

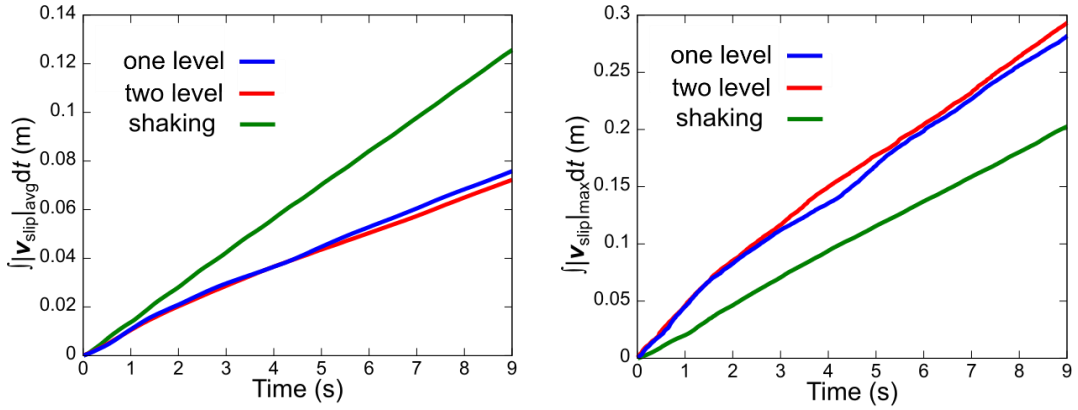

Fig. 6: Figure 6 Time variation of (a) averaged over all particles and (b) maximum slip velocity integrated in time.

the rotating velocity used was 60 rpm and mixing Reynolds number is

$$Re_{st} = \frac{d_I^{\,2}\omega}{\nu_f} = 1.008 \times 10^4 \quad (13)$$

$$Re_{sh} = \frac{2rR_s\omega}{\nu_f} = 5.998 \times 10^3 \quad (14)$$

The suffixes I, st and sh stand for impeller, stirring and shaking, respectively.

The slip velocity was defined as the velocity difference between the particle and the fluid and it was used to analyze the results obtained. As the slip velocity increases, the shear stress increases. The time variation of slip velocity averaged over all particles and the maximum slip velocity in the two cases of stirring and shaking are shown in **Figure 6.** Around *t* = 1.5 s, slope of the line of one-level and two-level impeller changes. This is due to the fact that the flow needs time to stabilize after the start of stirring. The results showed that the averaged slip velocity of one-level impeller integrated with time was larger than two-level while that of the two-level impeller exhibits higher the maximum slip velocity integrated in time than one-level. The averaged slip velocity for shaking is much larger than those for stirring, but the maximum slip velocity is much smaller than those for stirring. It is not yet fully understood how the average and the maximum shear stress affect the iPS cell suspension culture and which is more important for the control of the culture growth. Since the two types of mixing cause different shear stress distributions on the cell particles, the stirring or shaking should be used selectively depending on the application.

CONCLUSION

The present simulation results show that the slip velocity averaged over all particles of one-level impeller is larger than that of two-level. However, the maximum slip velocity of the two-level impeller is larger than that of one-level. Average shear stress produced during shaking is much larger than that for stirring, but the maximum shear stress

produced during shaking is much smaller than that for stirring. Therefore, stirring or shaking should be selectively used depending on the application. As a future work, other factors such as collision frequency and distribution must be investigated.

ACKNOWLEDGEMENTS

This research is partially supported by the project of "Development of Cell Production and Processing Systems for Commercialization of Regenerative Medicine" from Japan Agency for Medical Research and Development, AMED, and by a Grant-in-Aid for Scientific Research (B) (No. 15H04173) from the Ministry of Education, Culture, Sports, Science and Technology of Japan.

REFERENCES

1. Adamo, L., Naveiras, O., Wenzel, P.L., McKinney-Freeman, S., Mack, P.J., Gracia-Sancho, J., Sunchy-Dicey, A., Yoshimoto, M., Lensch, M.W., Yoder, M.C., Garcia-Cardena, G. and Daley, G.Q. (2009). Biomechanical forces promote embryonic haematopoiesis, *Nature.*, 459, 11311137.
2. Ali, B.A., Borner, M., Peglow, M., Janiga, G., Seidel-Morgenstern, A. and Thevenin, D. (2015). Coupled computational fluid dynamics-discrete element method simulations of a pilot-scale batch crystallizer, *Cryst. Growth Des.*, 15, 145155.
3. Issa, R.I. (1986). Solution of the implicitly discretized fluid flow equations by operator-splitting, *J. Comput. Phys.*, 62, 4065.
4. Jing, L., Kwok, C.Y., Leung, Y.F. and Sobral, Y.D. (2016). Extended CFD-DEM for free-surface flow with multi-size granules, *Int. J. Numer. Anal. Methods. Geomech.*, 40, 6279.
5. Olmer, R., Haase, A., Merkert, S., Cui, W., Palecek, J., Ran, C., Kirschning, A., Scheper, T., Glage, S., Miller, K., Curnow, E. C., Hayes, E.S. and Martin, U. (2010). Long term expansion of undifferentiated human iPS and ES cells in suspension culture using a defined medium, *Stem Cell Res.*, 5, 5164.
6. Olmer, R., Lage, S., Selzer, A., Kasper, C., Haverich, A., Martin, U. and Tomoda, K. (2012). Suspension culture of human pluripotent stem cells in controlled, stirred bioreactors, *J. Tissue. Eng.*, 18, 772784.
7. OpenFOAM; http://www.openfoam.com for the open source CFD tool box.
8. Otsuji, T.G., Bin, J., Yoshimura, A., Tomura, M., Tateyama, D., Minami, I., Yoshikawa, Y., Aiba, K., Heuser, J. E., Nishino, T., Hasegawa, K. and Nakatsuji, N. (2014). A 3D sphere culture system containing functional polymers for large-scale human pluripotent stem cell production, *Stem Cell Rep.*, 2, 734745.
9. Rusche, H. (2002). Computational fluid dynamics of dispersed two-phase flows at high phase fractions, *Ph. D. Thesis.*, Imperial College of Science, Technology and Medicine.
10. Salek, M.M., Sattari, P. and Martinuzzi, R.J. (2012). Analysis of fluid flow and wall shear stress patterns inside

partially filled agitated culture well plates, *Ann. Biomed. Eng.*, 40, 707728.

11. Sargent, C.Y., Berguig, G. Y., Kinney, M.A., Hiatt, L. A., Carpenedo, R.L., Berson, R.E. and McDevitt, T.C. (2010). Hydrodynamic modulation of embryonic stem cell differentiation by rotary orbital suspension culture, *Biotechnol. Bioeng.*, 105, 611626.
12. Takahashi, K., Tanabe, K., Ohnuki, M., Narita, M., Ichisaka, T., Tomoda, K. and Yamanaka, S. (2007). Induction of pluripotent stem cells from adult human fibroblasts by defined factors, *Cell.*, 131, 861872.
13. Zalc, J.M., Alvarez, M.M., Muzzio, F.J. and Arik, B.E. (2001). Extensive validation of computed laminar flow in a stirred tank with three rushton turbines, *Chem. Eng. Sci.*, 47, 21442154.